Non-Contact Imaging of Dielectric Constant with a Near-Field Scanning Microwave Microscope

Constantine P. Vlahacos, David E. Steinhauer, Steven M. Anlage, and Fred C. Wellstood, Department of Physics, University of Maryland, USA. Sudeep K. Dutta, University of California, Berkeley, USA. Johan B. Feenstra, Philips Res. Labs, Eindhoven, The Netherlands

Keywords: scanning probe microscopy, dielectric constant imaging, near-field microscopy

SUMMARY

We describe a non-contact technique for imaging dielectric constant using a resonant near-field scanning microwave microscope. By measuring the shift in the system's resonant frequency as we scan over an insulating sample, we obtain quantitative images of dielectric variations. We scanned seven samples with dielectric constants er ranging from 1 to 230, using a 480 μm diameter probe at a height of 100 μm and a frequency of 9.08 GHz. The technique achieves an accuracy of about 25% for ϵ_r=230 and less than 2% for ϵ_r=2.1, limited mainly by variations in the probe-sample separation.

INTRODUCTION

The ability to image variations in relative permittivity or dielectric constant er is useful for a variety of applications. For example, in thin-film microelectronics, testing for variations in dielectric constant can be used for quality control or to develop better growth techniques. As another example, knowledge of the dielectric constant at microwave frequencies is of great importance for the design of broadband circuits. Nowadays numerous techniques exist for measuring the dielectric constant and loss tangent of insulating materials at microwave frequencies [1-6]. However, most of these techniques involve working in contact and require thick homogeneous samples [1,2,4]. In this article, we report on the use of a resonant near-field scanning microwave microscope for the non-contact imaging of dielectric samples. Our approach offers a fast, simple, broadband method to image dielectrics using readily available microwave components.

Our resonant near-field scanning microwave microscope consists of a 1 m long coaxial transmission line which is capacitively coupled to a microwave source at one end and terminated by an open-ended coaxial probe at the other end. This arrangement creates a resonant circuit in which the resonant frequency f_0 and quality factor *Q* are modified when a sample approaches the open end of the probe (see inset in Fig. 1). By using a frequency-following feedback circuit we keep the microscope source locked on resonance [7]. We measure the shift of the system's resonant frequency Δf as we scan the sample under the probe. The variations in Δf are directly related to spatial variations in dielectric constant in the sample. In addition, however, topographic changes will also give rise to changes in Δf [8].

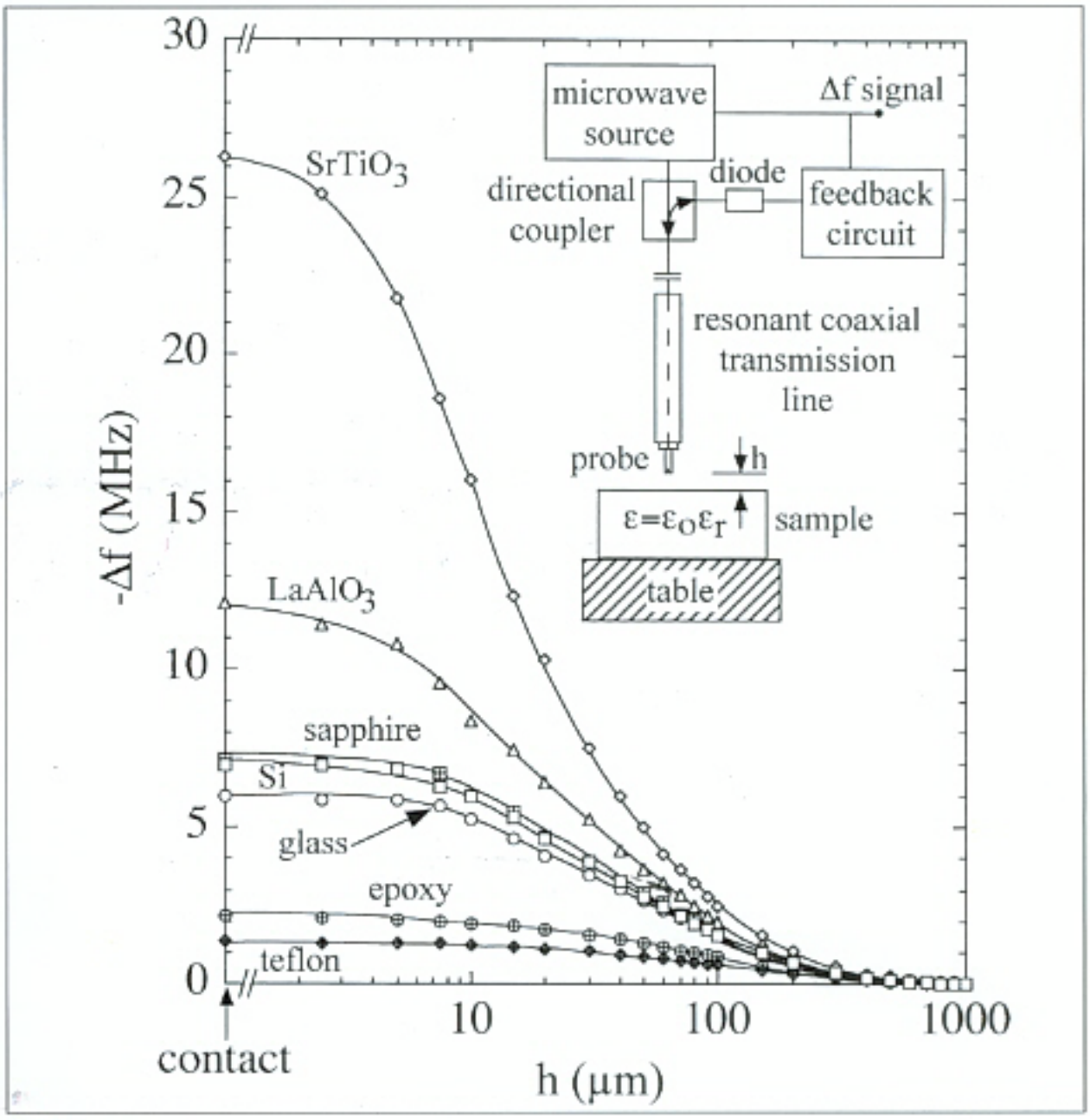

Figure1:
Frequency shift versus height for several dielectric samples measured at f_0=9.08 GHz with a 480 μm probe. Solid lines are guides to the eye. Inset shows schematic of the microwave microscope

CALIBRATION

To calibrate the system, we constructed a test sample by placing six pieces of different dielectric material into the bottom of a square plastic mould and pouring epoxy into the mould. In addition, silicone adhesive was used to hold each piece down. After the epoxy cured, the test sample was removed from the mould, polished, and positioned on the XY table. The materials embedded in the epoxy were silicon, glass microscope slide, $SrTiO_3$, Teflon, sapphire, and $LaAlO_3$. All six pieces were approximately 500 μm thick and about 6 mm x 8 mm in size. The overall thickness of the test sample was 6 mm.

We measured the frequency shift Δf versus height h above the six pieces, which have dielectric constants ranging from 2.1 to about

230. We also tested the epoxy which has an unknown dielectric constant. Each piece, as well as the probe, was flat and smooth on the scale of 5 μm as judged by an optical microscope. For these measurements, we used a probe with a 480 μm center conductor diameter and a source frequency of 9.08 GHz. For each scan, the probe was first brought in contact with a dielectric and the frequency shift Δf was recorded as the height was systematically increased. The results are plotted in Fig. 1. Samples with the largest dielectric constant produced the largest frequency shift, as expected. The largest shift we observed was -26.2 MHz, when the probe was in contact with a $SrTiO_3$ sample with ϵ_r=230 [9]. The smallest shift we found was -1.2 MHz when the probe was in contact with a Teflon sample with ϵ_r=2.1 [9]. As can be seen from Fig. 1, the frequency shift is essentially zero above 1 mm and saturates when the probe-sample distance is smaller than a few microns.

We used the above information to construct an empirical calibration curve that directly relates the frequency shift to the dielectric constanter. In order to construct the calibration curve we took the difference between the frequency shift at two different heights h_1 and h_2, i.e. $f_d=\Delta f(h_2)-\Delta f(h_1)$, where h_2 is far away (h_2>1000 μm). By taking the difference, we eliminated the effect of drift in the microwave source frequency. Proceeding this way for the test samples, we constructed two calibration curves of f_d versus ϵ_r (see Fig. 2), one curve for h_1=10 μm and h_2=1.1 mm and the other for h_1=100 μm and h_2=1.1 μm. We then set the parameters in each calibration curve with an empirical function (solid lines in Fig. 2), allowing us to easily transform any measured frequency shift to a dielectric constant. From these curves we can see that we can enhance the sensitivity to the dielectric constant considerably by using a small probe height. On the other hand, at closer probe-sample separations the influence of topographic features will be enhanced.

IMAGING RESULTS

To test the dielectric imaging capabilities of our system, we next scanned a single sample of $LaAlO_3$ which had an 8 x 5 mm triangular shape and a thickness of 510 μm. We placed the sample directly on the metal scanning table and recorded the frequency shift as a function of position. The data was taken at 9.08 GHz using the 480 μm probe at heights of 100 μm and 1.1 mm. We subtracted the two data sets and used our 100 μm calibration curve to transform the resulting frequency shift image into a dielectric constant image. Figure 3 shows the resulting contour image of dielectric constant versus position. The dielectric constant varies from about 20 to 25 over the sample and equals 1 when the probe is away from the sample. For comparison, the reported value of relative permittivity for $LaAlO_3$ at room temperature is ϵ_r=23.9 at 18 GHz [10]. In this image, the main variation in er over the sample is due to a slight tilt in the sample surface of about 20 μm. The edges of the sample show a smaller value of er due to averaging over the inner conductor of the probe. The width of the affected region is in good agreement with the expected spatial resolution of about 500 μm.

We next recorded a frequency shift image of the six-piece test sample using a probe-sample separation of 100 μm and the 480 μm diameter probe at 9.08 GHz. As before, using the $\epsilon_r(f_d)$ calibration, we then transformed the frequency shift image into a dielectric constant image (see Fig. 4a). The darker regions in Fig. 4a indicate a higher dielectric constant (larger frequency shift) and the lighter regions indicate a smaller dielectric constant (smaller frequency shift). Figure 4b shows the corresponding surface plot representation. Note that the z-axis in Fig. 4b uses a logarithmic scale to allow us to show the large range of dielectric constants present in the sample. As expected, the largest dielectric constant materials ($SrTiO_3$ and $LaAlO_3$) are the highest surfaces and the smallest dielectric constant materials (Teflon and vacuum) are the lowest. Further, notice that the Teflon sample forms a depression in Fig. 4b, indicating that the dielectric constant of Teflon is lower than the surrounding epoxy. We also note that voids in the epoxy can easily be seen as irregularly shaped low-dielectric regions (white regions

Table 1:
Experimental measurements of dielectric constant found at the centre of each material from Fig. 4 compared to literature values.

Material	Experimental value	Literature value	Frequency (GHz)	References
Silicon	12	11.7	100	11
Glass	12	6.7	10^{-3}	12
$SrTiO_3$	180	230	0.1	9
$LaAlO_3$	20	23.9	18	10
Sapphire (ceramic)	20	10.0	100	11
Teflon	2.1	2.1	10	9

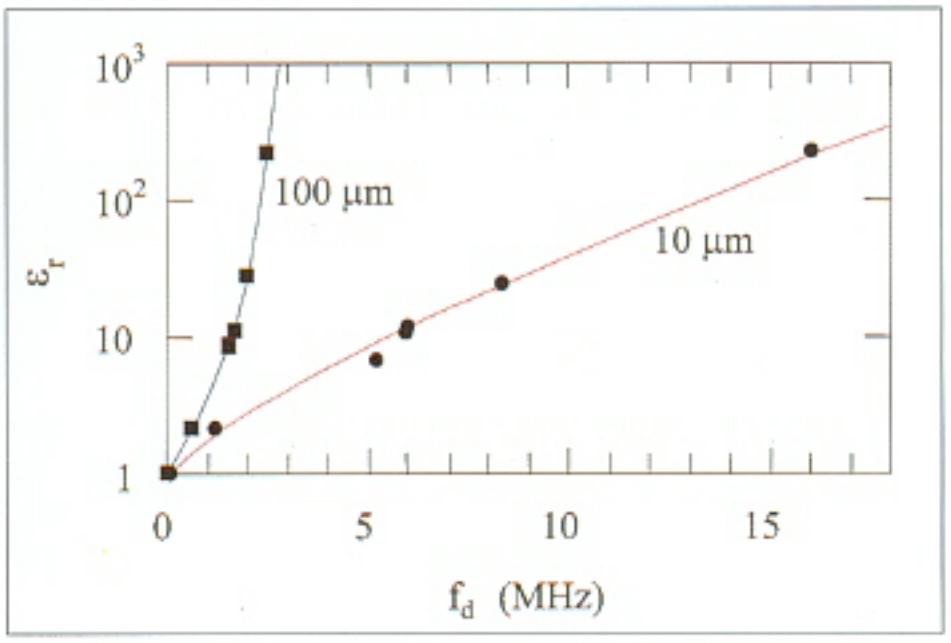

Figure 2:
Calibration curves of dielectric constant ϵ_r versus frequency shift f_d using a 480 μm probe at 9.08 GHz for closest approach heights of 100 μm and 10 μm.

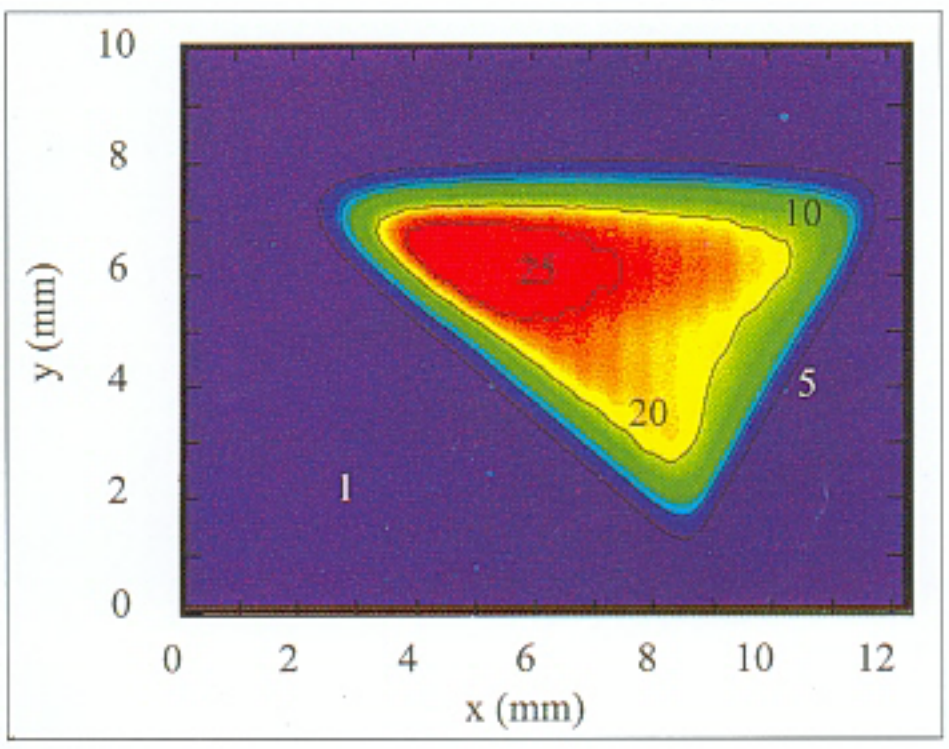

Figure 3:
Dielectric constant of $LaAlO_3$ sample imaged at 100 μm and 9.08 GHz using a 480 μm diameter probe. Contour lines are labelled with dielectric constant.

in Fig. 4a) in the epoxy. Table 1 summarizes the dielectric constants found from Fig. 4 for the six test materials.

From Fig. 4b, it is apparent that there is some noise in our images of dielectric constant. In our system, the predominant sources of random errors are noise in our recording electronics and fluctuations in the source frequency. To establish the precision to which ϵ_r can be determined, we determined the standard deviation in ϵ_r over a small region near the center of the $LaAlO_3$ sample in Fig. 3; we found $\Delta\epsilon_r$=0.06 for a sampling time of 30 ms. Similarly, over the Teflon in Fig. 4a the standard deviation in ϵ_r was $7x10^{-4}$ for a sampling time of 30 ms. From Fig. 4 we can also estimate the absolute accuracy of our technique. For ϵ_r=230 ($SrTiO_3$) the accuracy is about 25% while for ϵ_r=2.1 (Teflon) the accuracy is better than 2%. The main source of these errors is topographic variations. In our test sample, even after polishing, there are small height variations of about 30 μm (e.g. between the sapphire and $SrTiO_3$ in Fig. 4) between the different dielectrics. Such height variations cause an additional frequency shift [8], resulting in an error in the measured dielectric constant. In this regard, an accurate measurement of the dielectric constant of a single flat dielectric sample is considerably easier. However, the image of the composite sample clearly demonstrates the strength and sensitivity of this non-contact technique to measure variations in ϵ_r.

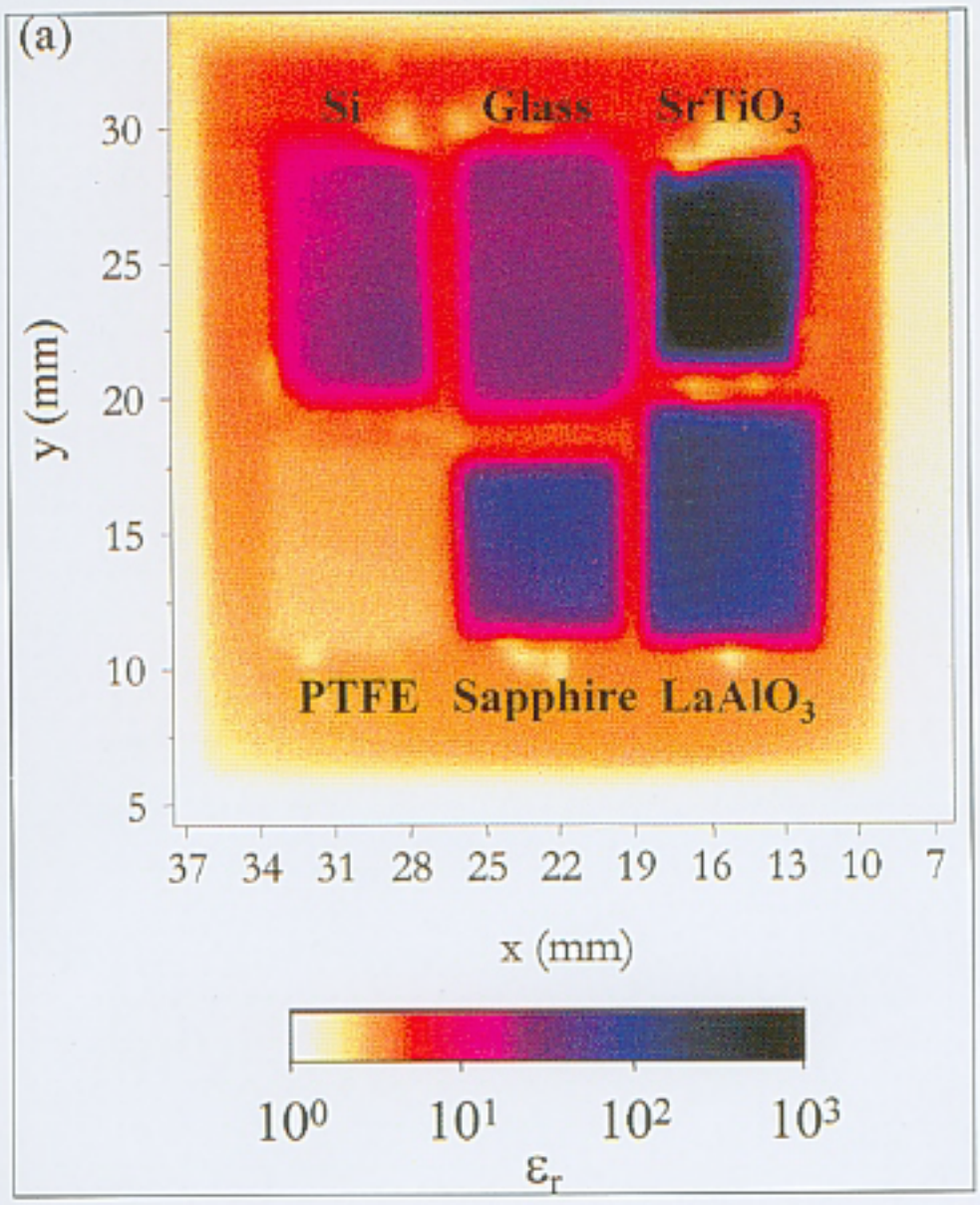

Figure 4a

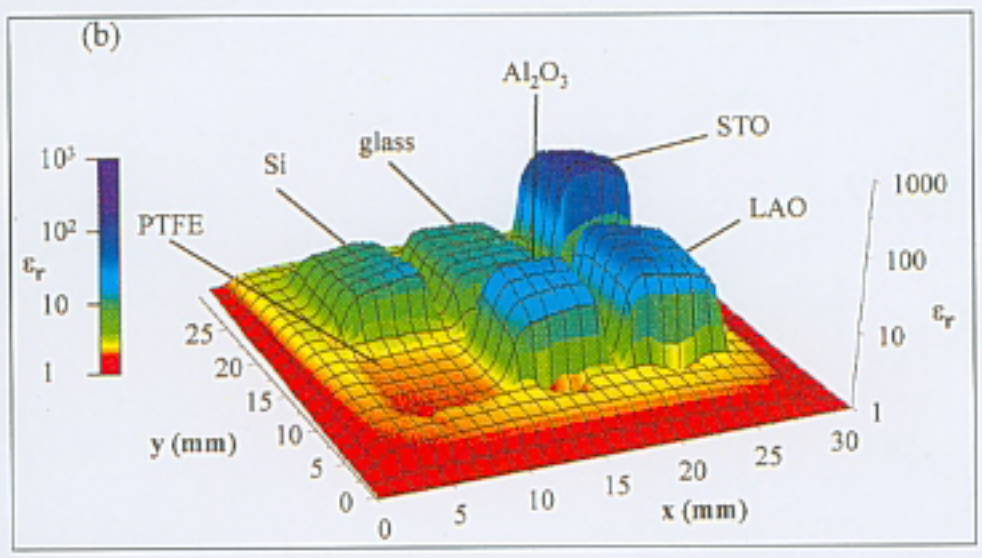

Figure 4b

Figure 4:
a: Dielectric constant image of a test sample taken with a 480 μm probe at 9.08 GHz and 100 μm above the sample. The materials used in the sample are, along the top row from left to right: silicon, glass, $SrTiO_3$; and along the bottom row from left to right: Teflon, sapphire, $LaAlO_3$.
b: Surface plot of the above sample on a logarithmic z-scale.

CONCLUSIONS

In summary, we have used an open-ended, resonant, near-field scanning microwave microscope to obtain quantitative images of the dielectric constant of bulk materials. Our system allows for fast, reliable, non-contact imaging of variations in the dielectric constant of flat samples, provided that the height of the probe above the sample is accurately controlled.

ACKNOWLEDGEMENTS

We acknowledge support from the National Science Foundation NSF-MRSEC grant No. DMR-9632521, NSF grant No. ECS-9632811, and from the Maryland Center for Superconductivity Research.

REFERENCES

1. *Tanabe E. and Joines W.T. A nondestructive method for measuring the complex permittivity of dielectric materials at microwave frequencies using an open transmission line resonator. IEEE Trans. Instrum. Meas. 25, 222-226, 1976.*
2. *Stuchly M.A. and Stuchly S. S., Coaxial line reflection methods for measuring dielectric properties of biological substances at radio and microwave frequencies-A Review. IEEE Trans. Instrum. Meas. 29, 176-183, 1980.*
3. *Wang M.S. and Borrego J. M. High-resolution scanning microwave electric-field probe for dielectric constant uniformity measurement. Materials Evaluation 48, 1106-1109, 1990.*
4. *Jiang G.Q. et al. Measurement of the microwave dielectric constant for low-loss samples with finite thickness using open-ended coaxial-line probes. Rev. Sci. Instrum. 64, 1622-1626, 1993.*
5. *Golosovsky M. and Davidov D. Novel millimeter-wave near-field resistivity microscope. Appl. Phys. Lett. 68, 1579-1581, 1996.*
6. *Lu Y. et al., Nondestructive imaging of dielectric-constant profiles and ferroelectric domains with a scanning-tip microwave near-field microscope. Science 276, 2004-2006,1997.*
7. *Steinhauer D.E. et al., Surface resistance imaging with a scanning near-field microwave microscope. Appl. Phys. Lett. 71, 1736-1738, 1997.*
8. *Vlahacos C.P. et al. Quantitative topographic imaging using a near-field scanning microwave microscope. Appl. Phys. Lett. 72, 1778-1780, 1998.*
9. *Ramo S. et al. Fields and Waves in Communication Electronics, P-285 3rd ed. Wiley, New York, 1994.*
10. *Zuccaro C. et al. Microwave absorption in single crystals of lanthanum aluminate. J. Appl. Phys. 82, 5695-5704, 1998.*
11. *Kozlov G. and Volkov A. In: Millimeter and Submillimeter Wave Spectroscopy of Solids, (eds. Grüner G. Dahl K. and Dahl C.) Topics in Applied Physics, 74, p. 261. Springer-Verlag, New York 1998.*
12. *Private communication with VWR Scientific, Inc.: the dielectric constant of Swiss Glass is ϵ_r=6.7*

Authors details: Constantine P. Vlahacos, Naval Surface Warfare Centre, Carderock Division, Code 67, 9500 MacArthur Boulevard, West Bethesda, Maryland 20817-5700 USA.
E-mail: vlahacos@nsweed.navy.mil
+1 301 227 4068